

TRANSLATIONAL SCIENCES



Atherosclerotic Plaque Epigenetic Age Acceleration Predicts a Poor Prognosis and Is Associated With Endothelial-to-Mesenchymal Transition in Humans

Ernest Diez Benavente¹,* Robin J.G. Hartman¹,* Tim R. Sakkars¹, Marian Wesseling¹, Yannicke Sloots, Lotte Slenders¹, Arjan Boltjes¹, Barend M. Mol¹, Gert J. de Borst¹, Dominique P.V. de Kleijn¹, Koen H.M. Prange¹, Menno P.J. de Winther¹, Johan Kuiper¹, Mete Civelek¹, Sander W. van der Laan¹, Steve Horvath, N. Charlotte Onland-Moret¹, Michal Mokry¹, Gerard Pasterkamp¹,* Hester M. den Ruijter*

BACKGROUND: Epigenetic age estimators (clocks) are predictive of human mortality risk. However, it is not yet known whether the epigenetic age of atherosclerotic plaques is predictive for the risk of cardiovascular events.

METHODS: Whole-genome DNA methylation of human carotid atherosclerotic plaques (n=485) and of blood (n=93) from the Athero-Express endarterectomy cohort was used to calculate epigenetic age acceleration (EAA). EAA was linked to clinical characteristics, plaque histology, and future cardiovascular events (n=136). We studied whole-genome DNA methylation and bulk and single-cell transcriptomics to uncover molecular mechanisms of plaque EAA. We experimentally confirmed our in silico findings using in vitro experiments in primary human coronary endothelial cells.

RESULTS: Male and female patients with severe atherosclerosis had a median chronological age of 69 years. The median epigenetic age was 65 years in females (median EAA, -2.2 [interquartile range, -4.3 to 2.2] years) and 68 years in males (median EAA, -0.3 [interquartile range, -2.9 to 3.8] years). Patients with diabetes and a high body mass index had higher plaque EAA. Increased EAA of plaque predicted future events in a 3-year follow-up in a Cox regression model (univariate hazard ratio, 1.7; $P=0.0034$) and adjusted multivariate model (hazard ratio, 1.56; $P=0.02$). Plaque EAA predicted outcome independent of blood EAA (hazard ratio, 1.3; $P=0.018$) and of plaque hemorrhage (hazard ratio, 1.7; $P=0.02$). Single-cell RNA sequencing in plaque samples from 46 patients in the same cohort revealed smooth muscle and endothelial cells as important cell types in plaque EAA. Endothelial-to-mesenchymal transition was associated with EAA, which was experimentally confirmed by *TGFβ*-triggered endothelial-to-mesenchymal transition inducing rapid epigenetic aging in coronary endothelial cells.

CONCLUSIONS: Plaque EAA is a strong and independent marker of poor outcome in patients with severe atherosclerosis. Plaque EAA was linked to mesenchymal endothelial and smooth muscle cells. Endothelial-to-mesenchymal transition was associated with EAA, which was experimentally validated. Epigenetic aging mechanisms may provide new targets for treatments that reduce atherosclerosis complications.

GRAPHIC ABSTRACT: A [graphic abstract](#) is available for this article.

Key Words: acceleration ■ endarterectomy ■ epigenomics ■ hemorrhage ■ muscle, smooth

Correspondence to: Hester M. den Ruijter, PhD, Division of Heart and Lungs, Department of Cardiology, Laboratory of Experimental Cardiology, Huispostnummer G03.550, PO Box 85500, 3508 GA Utrecht, the Netherlands. Email h.m.denruijter-2@umcutrecht.nl

*E. Diez Benavente, R.J.G. Hartman, G. Pasterkamp, and H.M. den Ruijter contributed equally.

Supplemental Material is available at <https://www.ahajournals.org/doi/suppl/10.1161/ATVBAHA.123.320692>.

For Sources of Funding and Disclosures, see page 1429.

© 2024 The Authors. *Arteriosclerosis, Thrombosis, and Vascular Biology* is published on behalf of the American Heart Association, Inc., by Wolters Kluwer Health, Inc.

This is an open access article under the terms of the [Creative Commons Attribution](#) License, which permits use, distribution, and reproduction in any medium, provided that the original work is properly cited.

Arterioscler Thromb Vasc Biol is available at www.ahajournals.org/journal/atvb

Nonstandard Abbreviations and Acronyms

EAA	epigenetic age acceleration
EC	endothelial cell
EndMT	endothelial-to-mesenchymal transition
IL	interleukin
scRNA-seq	single-cell RNA sequencing
SMC	smooth muscle cell

Chronological age is a strong predictor for morbidity and mortality. However, people age differently, which matured the concept of epigenetic age. The epigenetic age of a tissue can differ from the chronological age of the same individual. Biological age can be determined in multiple ways; one way is using the Horvath pan tissue clock¹ as an indicator for epigenetic age. In this method, DNA methylation levels at 353 CpG sites is used to predict chronological age. The predicted age estimate is referred to as epigenetic age or DNA methylation age. An age-adjusted measure of DNA methylation age, known as epigenetic age acceleration (EAA), is heritable (up to 40% in adults)² and predicts the prevalence and incidence of many leading diseases.³ In addition, EAA has been associated with poorer cardiovascular health.⁴

Atherosclerosis is the process in which lipids and immune cells accumulate and form a plaque in the subendothelial layer of the blood vessels.⁵ This plaque buildup underlies most cardiovascular diseases and is a long-term process that progresses during aging. We, therefore, hypothesize that plaque-specific epigenetic aging measured through DNA methylation reflects the progression of disease beyond chronological age.

Histology and imaging studies reveal that overall plaque burden is higher in men compared with women of similar age, and plaque phenotypes in men are associated with more inflammation and an unstable phenotype.⁶ With the well-known effects of sex hormones on epigenetic aging,^{7,8} we postulate that atherosclerotic plaques in women show delayed epigenetic aging compared with men.

We determined the epigenetic age of 485 atherosclerotic plaques and a subset of corresponding blood samples (n=93) using DNA methylation data. We evaluated the effect of epigenetic age, sex, and other risk factors on follow-up event rates of patients. Lastly, we studied the histological and molecular phenotypes underlying the EAA of plaques, using histopathologic assessment, epigenome-wide DNA methylation signatures, and single-cell RNA sequencing (scRNA-seq). In patients with advanced atherosclerotic disease, EAA of the plaque was marginally lower in women compared with men and associated with poorer clinical outcome. Plaque-specific EAA was associated with a large shift in genome-wide epigenetic and transcriptional states, which pointed

Highlights

- Epigenetic age acceleration of plaque, a measure of biological age, is a strong predictor of future events in patients with severe atherosclerosis.
- Epigenetic age differed between female and male plaques by 2 years and patients with diabetes and high body mass index presented with higher plaque epigenetic age acceleration.
- Epigenetic age acceleration in plaques coincided with endothelial-to-mesenchymal transition, a finding that was experimentally confirmed.

to mesenchymal reprogramming of smooth muscle cells (SMCs) and endothelial cells (ECs). The role of endothelial-to-mesenchymal transition (EndMT) in epigenetic aging was validated using *in vitro* experiments. Our data highlight the importance of epigenetic aging in atherosclerotic disease.

METHODS

Availability of Data

Anonymized data and materials have been made publicly available at DataverseNL and can be accessed at <https://doi.org/10.34894/4IKE3T>, <https://doi.org/10.34894/TYHGEEF>, and <https://doi.org/10.34894/D1MDKL>. The scripts that support the findings of this study are available from the corresponding author upon reasonable request.

Study Population

Athero-Express is an ongoing, prospective biobank study, collecting atherosclerotic plaques from patients undergoing carotid endarterectomy in 2 Dutch tertiary referral hospitals: University Medical Centre Utrecht and St. Antonius Hospital, Nieuwegein. The study design and inclusion criteria have been published previously.⁹ A baseline table for the 485 patients (148 women and 337 men) in this study is provided in [Data Set S1](#). These represented consecutive included patients between 2002 and 2011. Among these 485 patients who provided consent, 252 volunteered for additional blood donation for biomarker analysis. From this group of 252 patients, we measured blood DNA methylation on 93 randomly chosen individuals. We used the methylation data from these 93 patients as a reference for comparison to plaque DNA methylation. Indication for surgery was based on international guidelines for carotid and iliofemoral atherosclerotic disease,^{10–13} and standardized treatment protocols and operative techniques were applied. The medical ethics committees in both participating centers approved the study. All patients provided written informed consent. A composite cardiovascular end point for the outcome analysis of patients who underwent carotid endarterectomy was used. This consisted of (sudden) cardiovascular death, stroke, myocardial infarction, coronary intervention (coronary artery bypass grafting or percutaneous coronary intervention), peripheral re-intervention or leg amputation. For patients who reached multiple end points during follow-up, only the first manifestation of a

cardiovascular event was used for analysis of the composite end point. Censoring was used as a technique for the survival analysis to account for loss to follow-up.

Plaque Histopathology

As described previously,^{9,14–16} the atherosclerotic plaque was processed directly after surgery. According to a standardized protocol, the plaque was divided into segments of 5-mm thickness along the longitudinal axis. The segment with the greatest plaque burden was subjected to histological examination.⁹ Semiquantitative estimation of the plaque morphology was performed at $\times 40$ magnification for macrophage infiltration (CD68), SMC content (α -actin), amount of collagen (picosirius red), and calcification (hematoxylin and eosin). Histological plaque characteristics were scored as (1) no or minor staining or (2) moderate or heavy staining.⁹ For detailed explanation on the staining quantification, see [Supplemental Methods](#).

DNA Methylation Analysis

We used DNA methylation data from 485 atherosclerotic plaques and 93 overlapping blood samples, for which histological procedures, data collection, and normalization procedures were previously published.¹⁷ In brief, DNA was extracted from stored plaque segments and stored blood samples of patients using standardized in-house protocols as described before in the study by Van Der Laan et al.¹⁸ DNA purity and concentration were assessed using the Nanodrop 1000 system (Thermo Fisher Scientific, MA). DNA concentrations were equalized at 600 ng, randomized over 96-well plates, and bisulfite converted using a cycling protocol and the EZ-96 DNA methylation kit (Zymo Research, Orange County). Subsequently, DNA methylation was measured on Infinium HumanMethylation450 Beadchip Array (HM450k; Illumina, San Diego), which was performed at the Erasmus Medical Center Human Genotyping Facility in Rotterdam, the Netherlands. Processing of the sample and array was performed according to the manufacturer's protocol. We calculated epigenetic age using Horvath's clock with the R package cgager (v0.1.0, accessed from <https://github.com/metamaden/cgager>), which uses methylation values at 353 CpGs to generate a continuous value mimicking a person's epigenetic age. We calculated the EAA as the residual from a linear model: $\text{epigenetic age} \approx \text{chronological age}$. This analysis adjusts for the influence of chronological age on epigenetic age since both are heavily correlated. This method creates positive EAA values that indicate accelerated aging, whereas negative EAA values indicate decelerated aging.

The dimensionality reduction of 485 patient samples and B values of the DNA methylation data at 483 731 CpGs was performed using a t-distributed stochastic neighbor embedding with the *rtsne* package (v0.15). Differential methylation analysis was performed using *limma* (v3.46.0).¹⁹ We called a CpG with a Bonferroni-corrected $P < 0.05$ significantly differentially methylated. We used ChIPseeker²⁰ (v.1.26.2) to annotate the differentially methylated CpGs. Differentially methylated promoter CpGs were enriched using *clusterProfiler*.²¹

Atherosclerotic Plaque Transcriptome Analysis

In 420 of these plaques, we were able to collect methylation and RNA-sequencing data, which were processed

according to previously published methods.²² Briefly, the raw RNA-sequencing read counts were corrected for UMI (unique molecular identifiers) sampling.

$$\text{Corrected count} = -4096 \times \ln$$

Then these were normalized by sample sequencing depth and log-transformed. Differential gene expression analysis was performed using DESeq2²³ (v1.30.1). A gene was called differentially expressed if false discovery rate-adjusted P value was < 0.1 . Gene enrichment analysis was performed using *clusterProfiler* (v3.18.1),²¹ *enrichplot* (v1.10.2), and *enrichr*.²⁴

Statistical Analysis

All analyses were performed using R (v4.0.4) in R-Studio. Baseline tables were generated using the *tableone* package (accessed from <https://github.com/kaz-yos/tableone>). For comparison of 2 groups of continuous variables with normal distribution and equal variances, 2-tailed unpaired Student t tests were performed with a confidence level of 95%. Two-tailed unpaired Mann-Whitney U test with a confidence level of 95% was conducted if data were non-normally distributed. Linear models were constructed in R, adjusting for potential confounders when needed. Cox regressions, plotting, and adjusted Cox regressions were performed using *rms* (v6.2.0), *survminer* (v0.4.9), and *survival* (v3.2.10). Missing data were present for some cardiovascular risk factors (blood pressure, LDL [low-density lipoprotein], and HDL [high-density lipoprotein] cholesterol, and high-sensitivity C-reactive protein), which were not always documented in the electronic health records. All the variables that were used in the multivariate models were missing $< 10\%$, and, therefore, complete-case analyses were performed ([Data Set S2](#)).

Single-Cell RNA Sequencing

We used previously published scRNA-seq data of human atherosclerotic plaques,²⁵ as well as new data from the same cohort.²⁶ A total of 20 different cell clusters were identified from 46 patients. We used *addModuleScore* within *seurat*²⁷ to calculate module scores for genes highly expressed within accelerated plaques. This module score calculates the average expression levels of the genes differentially by EAA on a single-plaque cell level, subtracted by the aggregated expression of control gene sets. All analyzed genes are binned based on averaged expression, and the control genes are randomly selected from each bin.²⁸ Finally, we created violin plots to plot the obtained module scores over the different cell clusters.

In Vitro EndMT Model

The treatment of ECs with TGF- β and TNF- α has been described previously as a model for EndMT.^{29–31} Human coronary artery ECs (HCAECs) from 3 donors (donor 1: HCAECs, female, Lonza, lot number 19TL144559; donor 2: HCAECs, female, Lonza, lot number 20TL065655; donor 3: HCAECs, male, Lonza, Clonetics, 27662)³² were cultured until confluent. Cells were seeded in a 6-well plate with a concentration of 260 000 cells per well. After 24 hours of incubation (37 °C, 5% CO₂), cells were stimulated with either human TGF- β (10 ng/mL, catalog number 100-35B; Peprotech) or human TNF- α (10 ng/mL, catalog number 130-094-015; Miltenyi Biotec) or

a combination of TNF- α and TGF- β (both 10 ng/mL) in endothelial basal medium MV (Promocell; No. C-22220) with 0.5% fetal bovine serum (Corning; No. 35-079-CV). After 48 hours, the medium including stimuli was refreshed. DNA was isolated before stimulation (0 hours), after 48 hours of stimulation, and after 72 hours of stimulation. RNA was isolated at 0 and 72 hours. Microscopic pictures (EVOS; Thermo-Fisher Scientific) were taken on all timepoints to check morphology. For details on staining and RNA analysis in the in vitro EndMT model, please see [Supplemental Methods](#).

DNA Isolation and Quality Control

To isolate DNA, cells were resuspended in lysis buffer and proteinase K according to the Maxwell RSC Blood DNA Kit protocol (Maxwell; lot number 130384, reference AS1400) and isolated using the Promega Maxwell RSC instrument. DNA was quantified using the Qubit dsDNA HS assay kit (Thermo-Fisher Scientific; Q32854) on the Qubit Fluorometer (Thermo-Fisher). Total amount of DNA isolated from the samples ranged from 28.7 to 44.2 ng/ μ L. DNA purity was measured on Nanodrop (Thermo-Fisher). Three DNA samples were run on the electrophoresis gel to confirm the presence and quality of genomic DNA in the samples. Electrophoresis gel was made by heating and dissolving 1% agarose (Roche; 11388991001) in TAE (tris acetate ethylenediaminetetraacetic acid). Afterward, SYBR Safe DNA Gel Stain (Invitrogen; S33102) was added at 1:1000. Next, the gel was poured, and samples with 6 \times TriTrack DNA Loading Dye ratio 1:6 (Thermo Scientific; R1161) and a 1-kb plus DNA ladder (Invitrogen; 10787-018) were loaded. The gel ran on 70 to 80 V for around 45 minutes.

Methylation Data Generation and Analysis

Illumina Infinium MethylationEPIC v2.0 BeadChip was used to obtain DNA methylation profiles of 10 samples with DNA concentration of 11.8 ng/ μ L. This assay is based on bisulfite conversion. Data were generated at Genomic Centre, Erasmus Medical Centre, in Rotterdam, the Netherlands. Raw IDAT files were converted into the RGChannelSet object. Quality

control, normalization, and filtering were performed guided by the cross-package Bioconductor workflow31, using the Limma and Minfi packages. Probes with mean detection P value above 0.05 were removed ($n=0$). Normalization was performed with the preprocessQuantile function. Filtering criteria were applied as described in the Minfi package. Epigenetic aging was determined using Horvath clock with the R package cgager (v0.1.0, accessed from <https://github.com/metamaden/cgager>), which uses methylation values at 353 CpGs to generate a continuous value representing a sample's epigenetic age.

RESULTS

Chronological Age and Biological Plaque Age

To determine the epigenetic age of the atherosclerotic plaque, we used DNA methylation data of plaques from 485 patients (148 women and 337 men) who underwent a carotid endarterectomy. A baseline table with the clinical characteristics of the 485 patients is provided in [Data Set S1](#). Chronological age for the patients ranged from 40 to 91 years in females and 43 to 88 years in males, with a median age of 69 years for both sexes (Figure 1A). We used the Horvath pan tissue clock¹ since it applies to all nucleated cells including those found in plaques. Epigenetic age measured using the Horvath pan tissue clock ranged from 50.4 to 81.3 years of age for females, while it ranged from 51.0 to 88.8 years of age for males, with a median of 65.0 years for females, and of 67.6 years for males (Figure 1B). Chronological age of the patient and epigenetic age of atherosclerotic plaques were strongly correlated ($r=0.695$; $P=3.5\times 10^{-71}$; Figure 1C), indicating that the Horvath clock is relatively accurate in predicting age in diseased atherosclerotic tissue. We calculated EAA by taking the residuals of the linear model in which epigenetic age was predicted by chronological age. In this way, the resulting measure of age acceleration is independent of chronological age. A

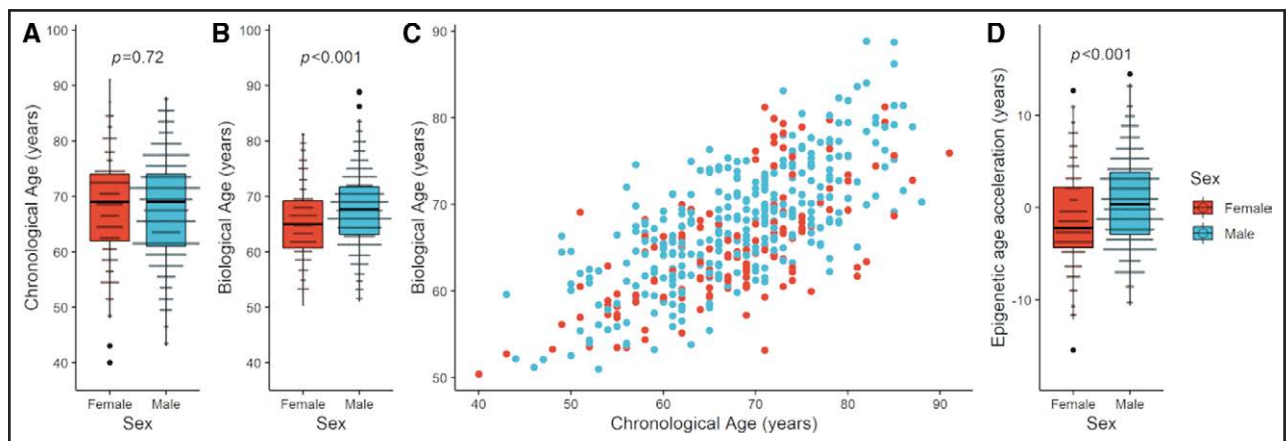


Figure 1. Chronological age vs plaque epigenetic age in 485 patients with carotid endarterectomy.

A, A boxplot shows the distribution and range of chronological age for the 485 patients in the study, stratified by sex. **B**, A boxplot shows the distribution and range of epigenetic age determined from DNA of 485 atherosclerotic plaques using the Horvath clock, stratified by sex. **C**, A scatterplot shows the strong correlation between chronological age (x axis) and epigenetic age (y axis), dots are color based on sex. **D**, A boxplot shows the distribution of range of epigenetic age acceleration, sex stratified.

negative EAA means that the chronological age is higher than the epigenetic age of the sample under study, which points to decelerated aging of the atherosclerotic plaque, whereas a positive EAA indicates accelerated aging of the plaque. EAA ranged from -15.4 to 12.6 years in females and from -10.6 to 14.4 years in males. The median EAA significantly differed between females and males by ≈ 2 years (females, -2.2 [interquartile range, -4.3 to 2.2] years versus males: 0.3 [interquartile range, -2.9 to 3.8] years; $P=5.99 \times 10^{-5}$; Figure 1D).

EAA Is Associated With Secondary Cardiovascular Events

Patients within the Athero-Express biobank are followed up for 3 years for secondary events (Methods). First, we performed a Cox regression on EAA and secondary composite events (Figure 2). To identify any risk factors

associated with EAA, we categorized our patient population into 2 groups, those with accelerated aging (EAA, >0 ; $n=224$) and those with decelerated aging (EAA, <0 ; $n=261$; Table). Importantly, since EAA is defined as the residual of the linear model specified above, chronological age is not different between the 2 groups. Notable differences between the groups are the number of males and females (accelerated, 80% male; decelerated, 60% male; $P<0.001$), their body mass index (accelerated, 27.1 ± 4.2 SD; decelerated, 26.1 ± 3.6 SD; $P=0.004$), and the presence of diabetes (accelerated, 26.8% diabetic; decelerated, 18.4% diabetic; $P=0.0035$). No other risk factors (plasma LDL, plasma HDL, hypertension, smoking, and high-sensitivity C-reactive protein [CRP]) significantly differed between patients with accelerated and decelerated plaque aging.

The association found between EAA and outcome did not substantially change when we corrected for sex,

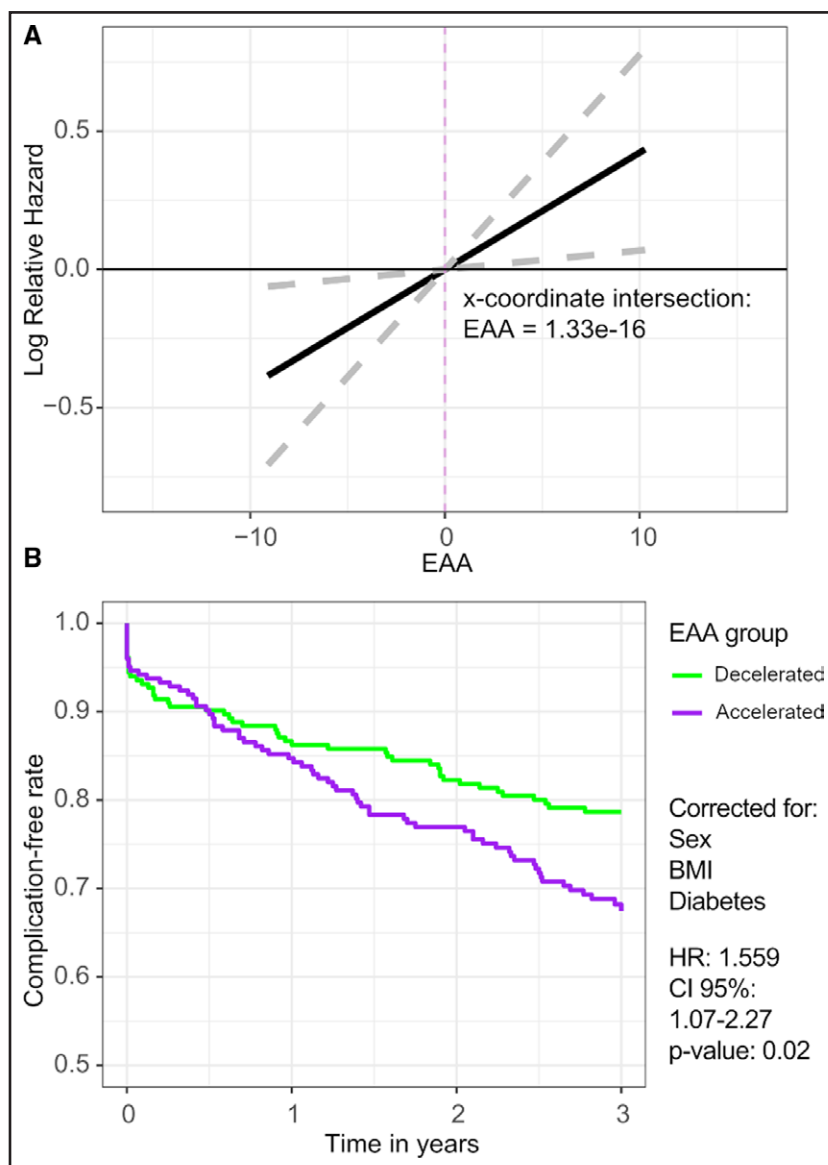


Figure 2. Epigenetic age acceleration (EAA) of carotid plaques and follow-up in 485 male and female patients with carotid endarterectomy.

A, A line graph portrays the relationship between the log of the relative hazard and EAA. The line intersects the y axis at $EAA=1.33 \times 10^{-16}$, indicated by the dashed purple line. Dashed gray lines indicate the CI. **B**, Cox regression survival graphs, adjusted for sex, body mass index (BMI), and diabetes, are shown for accelerated (purple) and decelerated (green) plaques. HR indicates hazard ratio.

Table. Baseline Table of Clinical Characteristics of Patients With Accelerated and Decelerated Plaques

Characteristic	Epigenetic age deceleration (n=261)	Epigenetic age acceleration (n=224)	P value
Chronological age, y	68 (9)	68 (9)	0.692
Smoking, yes (%)	102 (39.7)	92 (41.8)	0.705
Sex, male (%)	158 (60.5)	179 (79.9)	<0.001*
BMI, kg/m ² †	25.9 (24–28.3)	26.5 (24.5–29)	0.019*
Hypertension, yes (%)	224 (85.8)	201 (89.7)	0.244
Diabetes, yes (%)	48 (18.4)	60 (26.8)	0.035*
GFR CG, mL/min per 1.73 m ²	72 (59.9–90)	73 (53.6–90)	0.641
Systolic blood pressure, mm Hg	156 (26.4)	156 (25.5)	0.898
Diastolic blood pressure, mm Hg	83 (13)	82 (13.3)	0.384
Statin use, yes (%)	198 (75.9)	169 (75.4)	1
Dipyridamole use, yes (%)	135 (51.7)	105 (46.9)	0.33
Aspirin use, yes (%)	96 (36.8)	68 (30.4)	0.163
Contralateral stenosis, %			0.107
0–50	147 (60.0)	101 (48.6)	
50–70	27 (11.0)	31 (14.9)	
70–99	29 (11.8)	33 (15.9)	
100	42 (17.1)	43 (20.7)	
Symptoms, %			0.587
Asymptomatic	47 (18.1)	32 (14.3)	
Ocular	35 (13.5)	30 (13.4)	
Transient ischemic attack	115 (44.2)	98 (43.8)	
Stroke	63 (24.2)	64 (28.6)	
Plaque phenotype, %			0.093
Atheromatous	84 (32.2)	55 (24.6)	
Fibroatheromatous	104 (39.8)	89 (39.7)	
Fibrous	73 (28.0)	80 (35.7)	
Plaque hemorrhage, %	180 (69.2)	140 (62.5)	0.143
High-sensitivity CRP, mg/L	6.7 (14.3)	9.4 (18.1)	0.231
HDL, mmol/L†	1.1 (0.9–1.4)	1.1 (0.9–1.2)	0.282
LDL, mmol/L†	2.6 (2.1–3.4)	2.7 (2.2–3.6)	0.431

For continuous variables, the value is the average and in parenthesis is the SD; for categorical variables, the value represents counts and the parenthesis is the percentage. For non-normally distributed variables, the median and IQR are presented. BMI indicates body mass index; CRP, C-reactive protein; GFR CG, glomerular filtration rate (Cockcroft-Gault); HDL, high-density lipoprotein; IQR, interquartile range; and LDL, low-density lipoprotein.

*Significant differences.

†Non-normally distributed variables.

body mass index, and diabetes (adjusted Cox graphs; Figure 2B; hazard ratio [HR], 1.56; $P=0.02$). A multivariate Cox regression model was constructed for a subset of patients ($n=93$) where blood EAA was included as a confounding variable. This showed that the association

of plaque EAA with follow-up was independent of blood EAA (HR plaque EAA, 1.3; $P=0.018$; HR blood EAA, 0.1; $P=0.81$).

Interestingly, we observed a moderate correlation between plaque EAA and blood-based EAA across the subset of patients for whom both measurements were available (correlation coefficient, 0.44; $P<0.001$; $n=93$; Figure S2). There was no significant interaction between EAA and sex ($P=0.88$). As prognosis in these patients is associated with the presence of plaque hemorrhage,¹⁶ we studied whether EAA was specifically higher in plaques with plaque hemorrhage. However, plaque hemorrhage was not related with EAA, and adjustment for plaque hemorrhage of the Cox regression showed independent association for both plaque hemorrhage (HR, 1.6; $P=0.02$) and EAA (HR, 1.7; $P=0.007$) with secondary outcome.

Accelerated Aging Is Independent of Plaque Characteristics

As plaque-accelerated aging independently predicts cardiovascular secondary outcome, we tested whether this coincided with plaque phenotypes. The group with accelerated aging did not present with a specific plaque phenotype as semiquantitative hallmarks of plaque histology: fat, plaque hemorrhage, collagen, calcifications, SMC content, and macrophage content were not different (see Methods for staining procedures; Figure S3). Plaque overall phenotype (as shown in the Table) can be seen as a proxy for plaque cellular composition, which can significantly affect epigenetic age calculations.² Therefore, we investigated whether adjusting for plaque overall phenotype changed the results for secondary cardiovascular outcome. All analyses remained unchanged and significant, independently of plaque phenotype (HR, 1.6; $P=0.021$). These results prompted us to investigate the association of EAA with plaque biology at a molecular level by using genome-wide epigenetic signatures (beyond the 353 CpGs on which the EAA clock was built on) and gene expression patterns in accelerated and decelerated plaques.

EAA Is Associated With Changes in the Genome-Wide Epigenetic State in Human Plaques Beyond the Horvath Clock CpGs

The EAA has previously been described as a proxy for the state of the epigenetic maintenance system.¹ An accelerated aging in our case would indicate that the epigenetic machinery in the plaque has been under an increased biological workload. In contrast, a decelerated plaque aging would indicate that the epigenetic machinery has not been under a strong epigenetic maintenance influence as would be expected from plaques that are biologically less active.³³ We, therefore, studied whole-genome

DNA-methylation patterns in accelerated and decelerated aged plaques ($n=485$ male and female plaques). We excluded the epigenetic clock CpGs ($n=353$) from the DNA methylation analyses given that they are used to calculate the epigenetic age of plaques. Dimensionality reduction was performed on the remaining 483 731 CpGs (Figure 3A). We observed 2 large clusters representing male and female plaques in our cohort (Figure 3A). This clustering is likely driven by the differences in DNA methylation of the sex chromosomes: X inactivation leads to hypermethylation of many X chromosomal markers in females.^{34,35} Decelerated and accelerated aged plaques clustered separately within the female and to some extent, the male plaque groups (Figure 3A). Taking male and female plaques together, we found 65 488 differentially methylated CpGs between decelerated and accelerated aged plaques (Data Set S3). EAA was associated with hypermethylation of CpGs (45 287/65 488; Figure 3B). By using gene enrichment analysis on genes marked with differentially methylated CpGs in their promoter (within 1000 bases of the transcription start site), we found enrichment for SMC contraction and extracellular matrix organization. We found immune activation and cell adhesion enrichment for hypomethylated promoters of EAA plaques (Figure 3C). These enrichments were consistent in both female and male plaques when

stratifying by sex (Figure S4). We also studied enrichment of atherosclerotic pathways within the Horvath clock CpGs, but no signal was found for immune cell activation and SMC pathways. This is in line with previous results that highlighted that the processes enriched within the clock CpGs point to cell death/survival, cellular growth/proliferation, organismal/tissue development, and cancer.²

Transcriptional Changes in Epigenetically Accelerated Plaques Can Be Linked to Endothelial Cells and SMCs

To understand which molecular processes and cell types are actively involved during plaque EAA, we studied differential gene expression between accelerated and decelerated plaques using whole-plaque RNA sequencing. Of the 19 291 genes tested, 3031 were differentially expressed (false discovery rate, <0.1) between decelerated and accelerated plaques (Data Set S4). The majority of the differentially expressed genes were highly expressed in accelerated plaques (2839/3031 genes) as compared with decelerated plaques (Figure 4A). We found upregulated genes encoding for ribosomal proteins, as well as mitochondrial genes, in accelerated plaques. This points toward a general

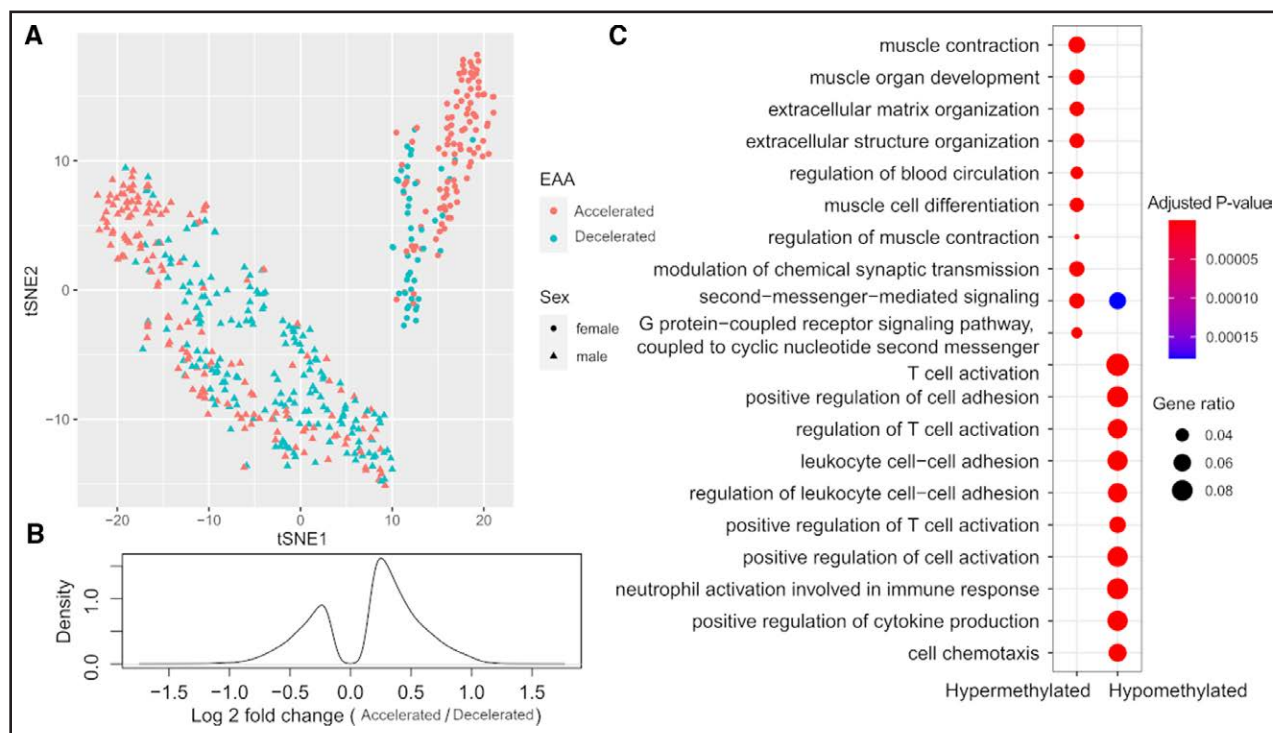


Figure 3. Epigenetic age acceleration (EAA) and DNA methylome of 485 male and female carotid plaques.

A, A t-distributed stochastic neighbor embedding (tSNE) plot is shown, reducing data of 485 samples based on project 483731 CG sites (CpGs) into 2 dimensions. Shape of the data point indicates sex; color indicates EAA group. We find visual evidence that females cluster into 2 separate groups that can be distinguished by EAA. **B**, A density plot shows the distribution of log₂-fold changes of all significant differentially methylated CpGs between accelerated and decelerated plaques. **C**, A dot plot shows the gene ontology biological process enrichment of promoter CpGs significantly hypermethylated and hypomethylated with accelerated epigenetic aging corrected for hospital of inclusion and sex. Color indicates significance of the enrichment, whereas size of the dot indicates gene ratio.

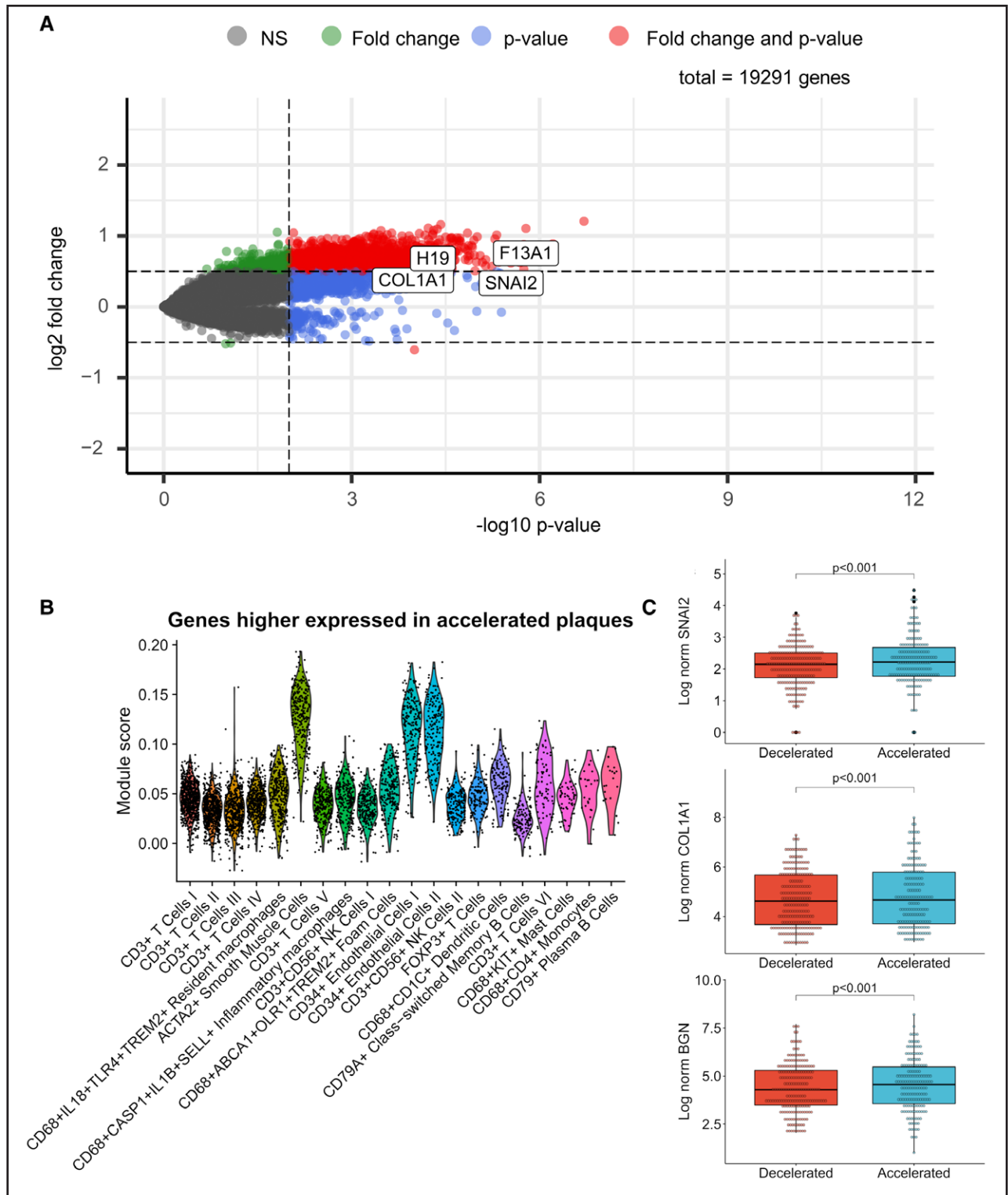


Figure 4. Epigenetic age acceleration and RNA transcriptome of 420 male and female carotid plaques.

A, An enhanced volcano plot is shown for the differential expression analysis between accelerated and decelerated plaques, where the x axis shows $-\log_{10}$ of the P value, and the y axis shows the log₂-fold change (accelerated over decelerated aging). Notable examples are highlighted in the plot by gene symbol. **B**, A violin plot shows the module score of genes higher expressed with accelerated aging from the bulk RNA sequencing over the single-cell clusters detected from the single-cell RNA sequencing of the human atherosclerotic plaque. Colors indicate different cell clusters. **C**, Boxplot of gene expression for epigenetically decelerated and accelerated plaques showing the genes of interest (*SNAI2*, *COL1A1*, and *BGN*). P values are determined using the DeSeq2 pipeline; normalized expression of the genes is obtained through the counts function in DeSeq2 package.

increase in translation turnover and mitochondrial respiratory activity within the plaque (Figure S5). Within the significantly upregulated genes, we identified 71 genes located within the coronary artery disease genome-wide association study loci,^{36,37} including among others *RAB23*, *C1S*, *COL4A2*, and *RPL17* (Data Set S4). Our epigenetic analyses of EAA suggest that gene regulation and translation is altered in plaque mesenchymal cells. With the knowledge that these cells display remarkable plasticity in atherosclerotic disease, we hypothesized that plaque EAA alters the transcriptional state of these cells. Therefore, we combined our whole-plaque RNA data set (420 patients, 127 women and 293 men) with single-cell RNA data from patients of the same cohort^{25,26} to project the plaque EAA genes over 20 single-cell clusters of the plaque. This includes 17 clusters of immune cells (macrophages, T cells, B cells, natural killer cells, and mast cells) and 3 clusters of mesenchymal cells (*ACTA2*⁺ SMCs and *CD34*⁺ ECs) within the plaque (4984 total cells from 46 patients, 20 women and 26 men).^{25,26} We generated a module score of the genes that were highly expressed in accelerated compared with decelerated plaques. We then projected this module score onto the individual cells within the 20 identified plaque cell clusters (Figure 4B). This module score was significantly higher in *ACTA2*⁺ SMCs (mean module score, 0.15) and the *CD34*⁺ EC clusters I and II (mean module scores, 0.12 for both) compared with the rest of the cells clusters within the plaque (mean module score, 0.02; all $P < 0.001$).

TGF β -Triggered EndMT Drives EAA in Coronary ECs

Within our study, we identified several known EndMT genes (ie, *SNAI2*, *COL1A1*; Figure 4C) among the differentially expressed genes between epigenetically accelerated and decelerated plaques. These genes were also mostly expressed in ECs and SMCs from atherosclerotic plaques (Figure S6). In addition, gene enrichment analysis using pathway databases (ie, MSigDB Hallmark 2020, Reactome, KEGG [Kyoto Encyclopedia of Genes and Genomes]) highlighted that genes upregulated in epigenetically accelerated plaques are involved in EndMT, TGF β signaling, TNF α signaling, and extracellular matrix-related processes (Figure 5A; Data Set S5). Furthermore, previous studies highlighted TGF β stimulation as an effector on epigenetics during EndMT.³⁸ This points to EndMT as potentially important in plaque EAA. The treatment of ECs with TGF- β and TNF- α has been described previously as a model for EndMT.^{29–31} To experimentally test whether EndMT drives epigenetic aging, we used a previously established EndMT protocol using human coronary artery ECs³¹ to study the effect of TGF β - and TNF α -triggered mesenchymal transition on epigenetic

aging (Figure 5B). Upon stimulation for 72 hours of coronary ECs with either TGF β , TNF α , or a combination of both (TGF β +TNF α) we observed a decrease in endothelial markers and an increase in the expression of mesenchymal markers, both at the protein level (Figure 5C) and at the gene expression level (Figure S7). We calculated the biological age by using the Horvath clock on genome-wide DNA methylation data before and after exposure. We observed a significant increase of 3.5 years ([95% CI, 0.06–6.9] $P=0.0072$) and 3.9 years ([95% CI, 0.04–7.4] $P=0.02$) in epigenetic age for both TGF β and TGF β +TNF α conditions, while no difference was found for the TNF α condition. Furthermore, no difference in epigenetic age was observed between the baseline and unstimulated condition (Figure 5D through 5G). These results further support that TGF β -triggered EndMT (independent of TNF α stimulation) is one of the drivers of epigenetic aging acceleration in atherosclerotic plaques.

DISCUSSION

We show that plaque EAA predicts outcome in patients with severe atherosclerotic disease. Plaques of women are epigenetically younger compared with men of the same age. Also, a high body mass index and the presence of diabetes was linked with epigenetically accelerated plaques. Multivariate analysis showed that EAA predicted secondary outcomes in patients independent of blood EAA, plaque hemorrhage, and other plaque phenotypes. This indicates that EAA is a strong biomarker for outcome, independent of the classical plaque paradigm of stable and unstable plaques. Interestingly, scRNA-seq analysis highlighted that mesenchymal endothelial cells and SMCs might be important cell types involved in plaque EAA. Gene enrichment analysis identified EndMT as an important process linked to EAA, which was experimentally confirmed by TGF β -triggered EndMT, which induced epigenetic aging in human coronary ECs.

Most studies thus far between survival and epigenetic age have been performed on systemic tissue, such as cells from blood. Our results on plaque EAA and outcome remained significant after adjusting for blood EAA within the same patients. This points that tissue specificity of the disease is an important characteristic, as described previously.^{39–41} We have identified such tissue-specific biomarkers in previous studies in this cohort, such as plaque FABP4 (fatty acid binding protein 4), which predicted secondary composite end points.⁴² Our in vitro experiments provide the first evidence that TGF β -induced EndMT promotes cellular aging of vascular cells. This further supports the relevance of EAA in vascular tissues. Previous studies have identified mitochondrial activity and cell plasticity (loss of stem-cell-like potential) as important in epigenetic aging in cells,³³ and these

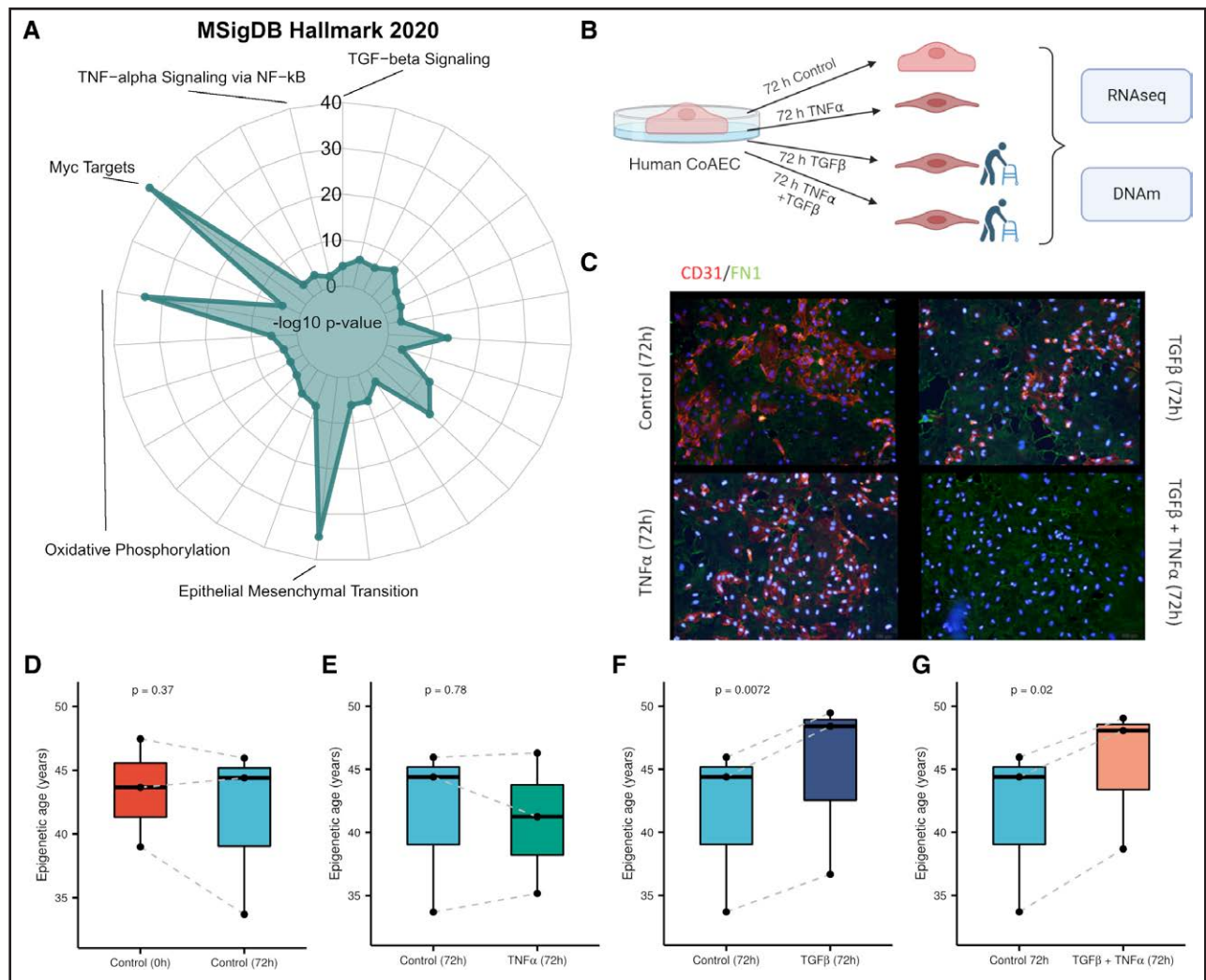


Figure 5. Epigenetic age acceleration is driven by endothelial-to-mesenchymal transition triggered by *TGFβ* (transforming growth factor beta).

A, Gene enrichment analysis of upregulated genes in plaque with accelerated epigenetic aging. **B**, Schematic of the in vitro stimulation of endothelial-to-mesenchymal transition using different stimuli identified in the enrichment analysis in **A**. **C**, Immunofluorescent staining of the human coronary artery endothelial cells under the different stimulation conditions; blue represents DAPI (4',6-diamidino-2-phenylindole) staining of nuclei. **D**, Epigenetic age (estimated using the Horvath clock) in control (no stimulation) at 0 hours and the control at 72 hours. **E**, Epigenetic age (estimated using the Horvath clock) in control at 72 hours and the *TNFα* (tumor necrosis factor alpha)-stimulated cells at 72 hours. **F**, Epigenetic age (estimated using the Horvath clock) in control at 72 hours and the *TGFβ*-stimulated cells at 72 hours. **G**, Epigenetic age (estimated using the Horvath clock) between the control at 72 hours and the *TGFβ*+*TNFα*-stimulated cells at 72 hours. CoAEC indicates coronary artery endothelial cells; DNAm, DNA methylation; FN1, fibronectin 1; MSigDB, Molecular Signatures Database; and RNA-seq, RNA sequencing.

processes were found to be upregulated in plaques epigenetically accelerated in this study.

Cells from the circulation can enter the plaque and become part of it, which may drive some of the epigenetic aging observed in this study. However, we found that the genes differentially expressed between accelerated and decelerated plaques were notably highly expressed in SMCs and ECs. These genes were not expressed by immune cells, which suggests that the observed plaque aging is not predominantly driven by circulating cells that infiltrate the plaque. Previous studies using circulating cells have shown that proinflammation pathways such

as IL (interleukin)-6, inflammasome, and IL-10 mediate the relationship between subclinical atherosclerosis and epigenetic age.⁴³ This is in line with our results showing that body mass index and diabetes associate with plaque epigenetic aging, as both risk factors are known to induce inflammatory pathways. For plaque tissue itself, the processes of epigenetic aging, however, seem to point toward mesenchymal cells.

We find a significant sex difference in plaque epigenetic age of around 2 years. This may be due to either a biological difference or driven by the Horvath clock itself. Previous studies have shown that the epigenetic age in

females is lower as compared with males when using the Horvath clock.⁷ An alternative explanation may be that females develop complications from atherosclerosis almost a decade later in life compared with men.⁴⁴ Although one may argue that this may be due to slower epigenetic aging in females, the absolute epigenetic age difference in our study is only 2 years which is too small to explain the observed sex differences in plaque phenotype and outcome.

We studied the epigenome, excluding the CpGs that comprise the Horvath clock, and found a marked difference in the epigenetics of plaques with EAA. We found enrichment for mesenchymal (hypomethylated) and immune processes (hypermethylated) in plaques with EAA. Our transcriptomic plaque data not only confirmed that inflammation and mesenchymal and fibrotic processes are at play but also highlight an increase in transcription activation and mitochondrial respiration. This suggests that plaques with accelerated aging may be more active, with both an inflammatory and mesenchymal component.

We experimentally tested the hypothesis that EndMT would be a driver of plaque EAA in coronary ECs. *TGFβ*-induced EndMT resulted in an increase of the epigenetic age of the cells. We found that this was independent of *TNFα* stimulation. Both *TGFβ*⁴⁵ and EndMT⁴⁶ have been implicated in atherosclerosis progression. It has been suggested that epigenetic age might be related to the loss of pluripotency by human cells.³³ Considering our experiments, it may be that transitioned ECs are in a permanent cell state and, therefore, have lost their pluripotency, which is reflected by their increased epigenetic age. The relationship between EAA and EndMT could also exist the other way around, where EAA could also influence EndMT. We did not explore this hypothesis in this study, but the interplay between cell plasticity and epigenetic aging warrants further studies.

Our study has several limitations. First, the RNA and DNA are from the same plaques but originate from different contiguous segments that may differ in cell content. Second, plaque EAA is not as easily obtainable as EAA from blood, which may limit the biomarker value for clinical practice. Nevertheless, it highlights mechanisms leading to accelerated aging and might help to understand their role in disease progression. Furthermore, plaques in our biobank are end stage, and our results may not be generalizable for earlier stages of atherosclerosis. Due to the limited sample size of our blood samples used to calculate blood EAA, we cannot make claims on the predictive power of blood EAA or on the comparison between blood and plaque EAA. Interestingly, other studies have shown that epigenetic age calculation from disease-relevant tissue has better prediction power than that of the readily available tissue.^{39–41} How relevant blood EAA is in predicting secondary cardiovascular events warrants further study in adequately blood sampled cohorts. The relationship between methylation and expression of nearby genes

is rather complex in plaque tissue, which is heterogeneous by nature. Therefore, we did not make statements on the direction of the gene expression changes caused by DNA methylation differences. Rather, we used this analysis to highlight the genes and pathways important for epigenetic aging. Finally, the limited plaque material did not allow us to study methylation and scRNA-seq in the same patients; therefore, different patient plaques of the same cohort were used. This may have caused selection bias. However, comparison of the 2 cohorts (DNA methylation and scRNA-seq) showed only small differences in patient and plaque characteristics, such as age and plaque hemorrhage. As women are known to have lower prevalence of plaque hemorrhage,⁴⁷ this difference between the subsets is likely driven by an intentional larger selection of female plaques in the scRNA-seq cohort. Despite this, the association between EAA and outcome was found independent of age, sex, and plaque hemorrhage in our multivariate Cox models and is, therefore, unlikely to change the EAA mechanisms identified in this study.

In conclusion, atherosclerotic plaque EAA is a strong and independent marker of a poor outcome in male and female patients with severe atherosclerosis. Plaque EAA transcriptional changes implicated mesenchymal endothelial cells and SMCs. EndMT was identified as a driver of EAA, which was experimentally confirmed. These epigenetic aging mechanisms may provide new targets for treatments that reduce the complications of atherosclerosis.

ARTICLE INFORMATION

Received January 8, 2024; accepted March 25, 2024.

Affiliations

Laboratory of Experimental Cardiology (E.D.B., R.J.G.H., T.R.S., Y.S., M.M., H.M.d.R.), Central Diagnostic Laboratory (M.W., L.S., A.B., S.W.v.d.L., M.M., G.P.), Julius Center for Health Sciences and Primary Care (N.C.O.-M.), and Department of Vascular Surgery (B.M.M., G.J.d.B., D.P.V.d.K.), University Medical Center Utrecht, Utrecht University, the Netherlands. Division of Biotherapeutics, Leiden Academic Centre for Drug Research, Leiden University, the Netherlands (K.H.M.P., M.P.J.d.W., J.K.). Center for Public Health Genomics (M.C.) and Department of Biomedical Engineering (M.C.), University of Virginia, Charlottesville. Department of Human Genetics, David Geffen School of Medicine (S.H.) and Department of Biostatistics, Fielding School of Public Health (S.H.), University of California, Los Angeles. Altos Labs, Cambridge Institute of Science, United Kingdom (S.H.).

Acknowledgments

The authors acknowledge the service of Single Cell Discoveries for single-cell RNA sequencing of human plaque material.

Sources of Funding

This study was funded by the European Union project European Research Council consolidator grant 866478 (UCARE), Leducq PlaQomics, and AtheroGEN.

Disclosures

None.

Supplemental Material

Supplemental Methods
Tables S1–S4
Figures S1–S7
References 48–52
Major Resource Table

REFERENCES

- Horvath S, Raj K. DNA methylation-based biomarkers and the epigenetic clock theory of ageing. *Nat Rev Genet*. 2018;19:371–384. doi: 10.1038/s41576-018-0004-3
- Horvath S. DNA methylation age of human tissues and cell types. *Genome Biol*. 2013;14:R115. doi: 10.1186/gb-2013-14-10-r115
- Hillary RF, Stevenson AJ, McCartney DL, Campbell A, Walker RM, Howard DM, Ritchie CW, Horvath S, Hayward C, McIntosh AM, et al. Epigenetic measures of ageing predict the prevalence and incidence of leading causes of death and disease burden. *Clin Epigenetics*. 2020;12:115. doi: 10.1186/s13148-020-00905-6
- Pottinger TD, Khan SS, Zheng Y, Zhang W, Tindle HA, Allison M, Wells G, Shadyab AH, Nassir R, Martin LW, et al. Association of cardiovascular health and epigenetic age acceleration. *Clin Epigenetics*. 2021;13:42. doi: 10.1186/s13148-021-01028-2
- Libby P, Buring JE, Badimon L, Hansson GK, Deanfield J, Bittencourt MS, Tokgözoğlu L, Lewis EF. Atherosclerosis. *Nat Rev Dis Prim*. 2019;5:56. doi: 10.1038/s41572-019-0106-z
- Man JJ, Beckman JA, Jaffe IZ. Sex as a biological variable in atherosclerosis. *Circ Res*. 2020;126:1297–1319. doi: 10.1161/CIRCRESAHA.120.315930
- Horvath S, Gurven M, Levine ME, Trumble BC, Kaplan H, Allayee H, Ritz BR, Chen B, Lu AT, Rickabaugh TM, et al. An epigenetic clock analysis of race/ethnicity, sex, and coronary heart disease. *Genome Biol*. 2016;17:0–22. doi: 10.1186/s13059-016-1030-0
- Sugrue VJ, Zoller JA, Narayan P, Lu AT, Ortega-Recalde OJ, Grant MJ, Bawden CS, Rudiger SR, Haghani A, Bond DM, et al. Castration delays epigenetic aging and feminizes DNA methylation at androgen-regulated loci. *Elife*. 2021;10:e64932. doi: 10.7554/eLife.64932
- Verhoeven BAN, Velema E, Schoneveld AH, Paul J, De Vries PM, De Bruin P, Seldenrijk CA, De Kleijn DPV, Busser E, Van Der Graaf Y, et al. Athero-Express: differential atherosclerotic plaque expression of mRNA and protein in relation to cardiovascular events and patient characteristics. Rationale and design. *Eur J Epidemiol*. 2004;19:1127–1133. doi: 10.1007/s10564-004-2304-6
- Norgren L, Hiatt WR, Dormandy JA, Nehler MR, Harris KA, Fowkes FGR, Bell K, Caporusso J, Durand-Zaleski I, Komori K, et al. Inter-society consensus for the management of peripheral arterial disease (TASC II). *Eur J Vasc Endovasc Surg Off J Eur Soc Vasc Surg*. 2007;33:S1–S75. doi: 10.1016/j.ejvs.2006.09.024
- European Carotid Surgery Trialists' Collaborative Group. Randomised trial of endarterectomy for recently symptomatic carotid stenosis: final results of the MRC European Carotid Surgery Trial (ECST). *Lancet*. 1998;351:1379–1387. doi: 10.1016/S0140-6736(97)09292-1
- Barnett HJ, Taylor DW, Eliasziw M, Fox AJ, Ferguson GG, Haynes RB, Rankin RN, Clagett GP, Hachinski VC, Sackett DL, et al. Benefit of carotid endarterectomy in patients with symptomatic moderate or severe stenosis. North American symptomatic carotid endarterectomy trial collaborators. *N Engl J Med*. 1998;339:1415–1425. doi: 10.1056/NEJM199811123392002
- Halliday A, Mansfield A, Marro J, Peto C, Peto R, Potter J, Thomas D; MRC Asymptomatic Carotid Surgery Trial (ACST) Collaborative Group. Prevention of disabling and fatal strokes by successful carotid endarterectomy in patients without recent neurological symptoms: randomised controlled trial. *Lancet*. 2004;363:1491–1502. doi: 10.1016/S0140-6736(04)16146-1
- de Bakker M, Timmerman N, van Koevorden ID, de Kleijn DPV, de Borst GJ, Pasterkamp G, Boersma E, den Ruijter HM. The age- and sex-specific composition of atherosclerotic plaques in vascular surgery patients. *Atherosclerosis*. 2020;310:1–10. doi: 10.1016/j.atherosclerosis.2020.07.016
- Van Koevorden ID, de Bakker M, Haitjema S, Van Der Laan SW, De Vries JPPM, Hoefler IE, De Borst GJ, Pasterkamp G, Den Ruijter HM. Testosterone to oestradiol ratio reflects systemic and plaque inflammation and predicts future cardiovascular events in men with severe atherosclerosis. *Cardiovasc Res*. 2019;115:453–462. doi: 10.1093/cvr/cvy188
- Hellings WE, Peeters W, Moll FL, Piers SRD, van Setten J, Van der Spek PJ, de Vries JPPM, Seldenrijk KA, De Bruin PC, Vink A, et al. Composition of carotid atherosclerotic plaque is associated with cardiovascular outcome: a prognostic study. *Circulation*. 2010;121:1941–1950. doi: 10.1161/CIRCULATIONAHA.109.887497
- Siemelink MA, van der Laan SW, Haitjema S, van Koevorden ID, Schaap J, Wesseling M, de Jager SCA, Mokry M, van IJterson M, Dekkers KF, et al. Smoking is associated to DNA methylation in atherosclerotic carotid lesions. *Circ Genomic Precis Med*. 2018;11:e002030. doi: 10.1161/CIRCGEN.117.002030
- Van Der Laan SW, Foroughi Asl H, van den Borne P, van Setten J, van der Perk MEM, van de Weg SM, Schoneveld AH, de Kleijn DPV, Michoel T, Björkregren JLM, et al. Variants in ALOX5, ALOX5AP and LTA4H are not associated with atherosclerotic plaque phenotypes: the Athero-Express Genomics Study. *Atherosclerosis*. 2015;239:528–538. doi: 10.1016/j.atherosclerosis.2015.01.018
- Ritchie ME, Phipson B, Wu D, Hu Y, Law CW, Shi W, Smyth GK. Limma powers differential expression analyses for RNA-sequencing and microarray studies. *Nucleic Acids Res*. 2015;43:e47. doi: 10.1093/nar/gkv007
- Yu G, Wang L, He Q. ChIPseeker: an R/Bioconductor package for ChIP peak annotation, comparison and visualization. *Bioinformatics*. 2015;31:2382–2383. doi: 10.1093/bioinformatics/btv145
- Yu G, Wang LG, Han Y, He QY. clusterProfiler: an R package for comparing biological themes among gene clusters. *Omi A J Integr Biol*. 2012;16:284–287. doi: 10.1089/omi.2011.0118
- Mokry M, Boltjes A, Slenders L, Bel-Bordes G, Cui K, Brouwer E, Mekke JM, Depuydt MAC, Timmerman N, Waissi F, et al. Transcriptomic-based clustering of human atherosclerotic plaques identifies subgroups with different underlying biology and clinical presentation. *Nat Cardiovasc Res*. 2022;1:1140–1155. doi: 10.1038/s44161-022-00171-0
- Love MI, Huber W, Anders S. Moderated estimation of fold change and dispersion for RNA-seq data with DESeq2. *Genome Biol*. 2014;15:550. doi: 10.1186/s13059-014-0550-8
- Chen EY, Tan CM, Kou Y, Duan Q, Wang Z, Meirelles GV, Clark NR, Ma'ayan AE. interactive and collaborative HTML5 gene list enrichment analysis tool. *BMC Bioinf*. 2013;14:128. doi: 10.1186/1471-2105-14-128
- Depuydt MA, Prange KH, Slenders L, Örd T, Elbersen D, Boltjes A, de Jager SC, Asselbergs FW, de Borst GJ, Aavik E, et al. Microanatomy of the human atherosclerotic plaque by single-cell transcriptomics. *Circ Res*. 2020;127:1437–1455. doi: 10.1161/CIRCRESAHA.120.316770
- Diez Benavente E, Karnewar S, Buono M, Mili E, Hartman RJG, Kapteijn D, Slenders L, Daniels M, Aherrahrou R, Reinberger T, et al. Female gene networks are expressed in myofibroblast-like smooth muscle cells in vulnerable atherosclerotic plaques. *Arterioscler Thromb Vasc Biol*. 2023;43:1836–1850. doi: 10.1161/ATVBAHA.123.319325
- Butler A, Hoffman P, Smibert P, Papalexli E, Satija R. Integrating single-cell transcriptomic data across different conditions, technologies, and species. *Nat Biotechnol*. 2018;36:411–420. doi: 10.1038/nbt.4096
- Tirosh I, Izar B, Prakadan SM, Wadsworth MH 2nd, Treacy D, Trombetta JJ, Rotem A, Rodman C, Lian C, Lian C, Murphy G, et al. Dissecting the multicellular ecosystem of metastatic melanoma by single-cell RNA-seq. *Science*. 2016;352:189–196. doi: 10.1126/science.aad0501
- Zeisberg EM, Tarnavski O, Zeisberg M, Dorfman AL, McMullen JR, Gustafsson E, Chandraker A, Yuan X, Pu WT, Roberts AB, et al. Endothelial-to-mesenchymal transition contributes to cardiac fibrosis. *Nat Med*. 2007;13:952–961. doi: 10.1038/nm1613
- Yoshimatsu Y, Wakabayashi I, Kimuro S, Takahashi N, Takahashi K, Kobayashi M, Maishi N, Podyma-Inoue KA, Hida K, Miyazono K, et al. TNF- α enhances TGF- β -induced endothelial-to-mesenchymal transition via TGF- β signal augmentation. *Cancer Sci*. 2020;111:2385–2399. doi: 10.1111/cas.14455
- Slenders L, Wesseling M, Boltjes A, Kapteijn DMC, Depuydt MAC, Prange K, van den Dungen NAM, Benavente ED, de Kleijn DPV, et al. Identification of endothelial-to-mesenchymal transition gene signatures in single-cell transcriptomics of human atherosclerotic tissue. *bioRxiv*. Preprint posted online July 18, 2023. doi: 10.1101/2023.07.18.549599
- Haitjema S, Meddens CA, van der Laan SW, Kofink D, Harakalova M, Tragante V, Foroughi Asl H, van Setten J, Brandt MM, Bis JC, et al. Additional candidate genes for human atherosclerotic disease identified through annotation based on chromatin organization. *Circ Cardiovasc Genet*. 2017;10:e001664. doi: 10.1161/CIRCGENETICS.116.001664
- Kabacik S, Lowe D, Fransen L, Leonard M, Ang SL, Whiteman C, Corsi S, Cohen H, Felton S, Bali R, et al. The relationship between epigenetic age and the hallmarks of aging in human cells. *Nat Aging*. 2022;2:484–493. doi: 10.1038/s43587-022-00220-0
- McCarthy MM, Auger AP, Bale TL, De Vries GJ, Dunn GA, Forger NG, Murray EK, Nugent BM, Schwarz JM, Wilson ME. The epigenetics of sex differences in the brain. *J Neurosci*. 2009;29:12815–12823. doi: 10.1523/JNEUROSCI.3331-09.2009
- Liu J, Morgan M, Hutchison K, Calhoun VD. A study of the influence of sex on genome wide methylation. *PLoS One*. 2010;5:e10028. doi: 10.1371/journal.pone.0010028
- Erdmann J, Kessler T, Munoz Venegas L, Schunkert H. A decade of genome-wide association studies for coronary artery disease: the challenges ahead. *Cardiovasc Res*. 2018;114:1241–1257. doi: 10.1093/cvr/cvy084
- Aragam KG, Jiang T, Goel A, Kanoni S, Wolford BN, Atri DS, Weeks EM, Wang M, Hindy G, Zhou W, et al; Biobank Japan. Discovery and systematic characterization of risk variants and genes for coronary artery

- disease in over a million participants. *Nat Genet.* 2022;54:1803–1815. doi: 10.1038/s41588-022-01233-6
38. Cardenas H, Vieth E, Lee J, Segar M, Liu Y, Nephew KP, Matei D. TGF- β induces global changes in DNA methylation during the epithelial-to-mesenchymal transition in ovarian cancer cells. *Epigenetics.* 2014;9:1461–1472. doi: 10.4161/15592294.2014.971608
 39. Levine ME, Lu AT, Bennett DA, Horvath S. Epigenetic age of the pre-frontal cortex is associated with neuritic plaques, amyloid load, and Alzheimer's disease related cognitive functioning. *Aging (Albany NY).* 2015;7:1198–1211. doi: 10.18632/aging.100864
 40. Horvath S, Oshima J, Martin GM, Lu AT, Quach A, Cohen H, Felton S, Matsuyama M, Lowe D, Kabacik S, et al. Epigenetic clock for skin and blood cells applied to Hutchinson Gilford progeria syndrome and ex vivo studies. *Aging (Albany NY).* 2018;10:1758–1775. doi: 10.18632/aging.101508
 41. Sillanpää E, Heikkinen A, Kankaanpää A, Paavilainen A, Kujala UM, Tammelin TH, Kovanen V, Sipilä S, Pietiläinen KH, Kaprio J, et al. Blood and skeletal muscle ageing determined by epigenetic clocks and their associations with physical activity and functioning. *Clin Epigenetics.* 2021;13:110. doi: 10.1186/s13148-021-01094-6
 42. Peeters W, de Kleijn DPV, Vink A, van de Weg S, Schoneveld AH, Sze SK, van der Spek PJ, de Vries JPPM, Moll FL, Pasterkamp G. Adipocyte fatty acid binding protein in atherosclerotic plaques is associated with local vulnerability and is predictive for the occurrence of adverse cardiovascular events. *Eur Heart J.* 2011;32:1758–1768. doi: 10.1093/eurheartj/ehq387
 43. Sánchez-Cabo F, Fuster V, Silla-Castro JC, González G, Lorenzo-Vivas E, Alvarez R, Callejas S, Benguría A, Gil E, Núñez E, et al. Subclinical atherosclerosis and accelerated epigenetic age mediated by inflammation: a multi-omics study. *Eur Heart J.* 2023;44:2698–2709. doi: 10.1093/eurheartj/ehad361
 44. Townsend N, Wilson L, Bhatnagar P, Wickramasinghe K, Rayner M, Nichols M. Cardiovascular disease in Europe: epidemiological update 2016. *Eur Heart J.* 2016;37:3232–3245. doi: 10.1093/eurheartj/ehw334
 45. Chen PY, Qin L, Li G, Wang Z, Dahlman JE, Malagon-Lopez J, Gujja S, Cilfone NA, Kauffman KJ, Sun L, et al. Endothelial TGF- β signalling drives vascular inflammation and atherosclerosis. *Nat Metab.* 2019;1:912–926. doi: 10.1038/s42255-019-0102-3
 46. Evrard SM, Lecce L, Michelis KC, Nomura-Kitabayashi A, Pandey G, Purushothaman KR, d'Escamard V, Li JR, Hadri L, Fujitani K, et al. Endothelial to mesenchymal transition is common in atherosclerotic lesions and is associated with plaque instability. *Nat Commun.* 2016;7:11853. doi: 10.1038/ncomms11853
 47. Vrijenhoek JEP, Den Ruijter HM, De Borst GJ, de Kleijn DPV, De Vries JPPM, Bots ML, Van de Weg SM, Vink A, Moll FL, Pasterkamp G. Sex is associated with the presence of atherosclerotic plaque hemorrhage and modifies the relation between plaque hemorrhage and cardiovascular outcome. *Stroke.* 2013;44:3318–3323. doi: 10.1161/STROKEAHA.113.002633
 48. Schwartz SM, Galis ZS, Rosenfeld ME, Falk E. Plaque rupture in humans and mice. *Arterioscler Thromb Vasc Biol.* 2007;27:705–713. doi: 10.1161/01.ATV.0000261709.34878.20
 49. Lusby RJ, Ferrell LD, Ehrenfeld WK, Stoney RJ, Wylie EJ. Carotid plaque hemorrhage. Its role in production of cerebral ischemia. *Arch Surg.* 1982;117:1479–1488. doi: 10.1001/archsurg.1982.01380350069010
 50. Davies MJ, Richardson PD, Woolf N, Katz DR, Mann J. Risk of thrombosis in human atherosclerotic plaques: role of extracellular lipid, macrophage, and smooth muscle cell content. *Br Heart J.* 1993;69:377–381. doi: 10.1136/hrt.69.5.377
 51. Hashimshony T, Senderovich N, Avital G, Klochendler A, de Leeuw Y, Anavy L, Gennert D, Li S, Livak KJ, Rozenblatt-Rosen O, et al. CEL-Seq2: sensitive highly multiplexed single-cell RNA-seq. *Genome Biol.* 2016;17:77. doi: 10.1186/s13059-016-0938-8
 52. Gu Z, Eils R, Schlesner M. Complex heatmaps reveal patterns and correlations in multidimensional genomic data. *Bioinformatics.* 2016;32:2847–2849. doi: 10.1093/bioinformatics/btw313